Protease-Sensitive Scrapie Prion Protein in Aggregates of Heterogeneous Sizes†

Salit Tzaban,‡ Gilgi Friedlander,‡ Oshrat Schonberger,‡ Lior Horonchik,‡ Yifat Yedidia,‡ Gideon Shaked,§ Ruth Gabizon,§ and Albert Taraboulos*,‡

Department of Molecular Biology, The Hebrew University−Hadassah Medical School, and Department of Neurology, Hadassah University Hospital, Jerusalem 91120, Israel

Received April 12, 2002; Revised Manuscript Received July 11, 2002

ABSTRACT: The pathological prion protein PrP^{Sc} is the only known component of the infectious prion. In cells infected with prions, PrP^{Sc} is formed posttranslationally by the refolding of the benign cell surface glycoprotein PrP^{C} into an aberrant conformation. The two PrP isoforms possess very different properties, as PrP^{Sc} has a protease-resistant core, forms very large amyloidic aggregates in detergents, and is only weakly immunoreactive in its native form. We now show that prion-infected rodent brains and cultured cells contain previously unrecognized protease-sensitive PrP^{Sc} varieties. In both ionic (Sarkosyl) and nonionic (*n*-octyl β-D-glucopyranoside) detergents, the novel protease-sensitive PrP^{Sc} species formed aggregates as small as 600 kDa, as measured by gel filtration. The denaturation dependence of PrP^{Sc} immunoreactivty correlated with the size of the aggregate. The small PrP^{Sc} aggregates described here are consistent with the previous demonstration of scrapie infectivity in brain fractions with a sedimentation coefficient as small as 40 S [Prusiner et al. (1980) *J. Neurochem. 35*, 574−582]. Our results demonstrate for the first time that prion-infected tissues contain protease-sensitive PrP^{Sc} molecules that form low MW aggregates. Whether these new PrP^{Sc} species play a role in the biogenesis or the pathogenesis of prions remains to be established.

The transmissible spongiform encephalopathies (TSE)[1] such as Creutzfeldt−Jakob disease of humans and scrapie of sheep are caused by prions (*1*) (for reviews, see *2*−*4*). TSE prions seem to propagate by refolding the membrane glycoprotein PrP^{C} into a pathogenic 'prion' conformation termed PrP^{Sc}, which in turn is their only known component (*5*, *6*). These two PrP isoforms thus possess the same covalent structure (*7*), but differ in their conformation as PrP^{Sc} is enriched in β-sheets (*8*, *9*) while PrP^{C} is predominantly α-helical. PrP^{C} is a copper binding protein (*10*) that is anchored to the surface of a variety of cells through a GPI moiety (*11*).

While understanding PrP^{C} and PrP^{Sc} is cardinal to prion biology, it is often difficult to distinguish between these two isoforms. Originally, PrP^{Sc} denoted the PrP species copurifying with scrapie infectivity (*12*, *13*), but this definition has been largely supplanted by biochemical criteria that were found to discriminate between PrP^{C} and PrP^{Sc}. Seminal studies conducted with the Sc237 strain of experimental scrapie in Syrian hamsters (*14*) showed that the two PrP isoforms possess very different biochemical properties. In contrast to PrP^{C}, PrP^{Sc} (i) is insoluble in nondenaturing detergents, (ii) possesses a core (called PrP27−30) which partially resists nonspecific proteolysis, and (iii) polymerizes into very large amyloidic structures (called prion rods) under the combined action of proteases and detergents (*15*, *16*). Prion rods contain as many as 3×10^4 PrP molecules. These biochemical attributes of PrP^{C} and PrP^{Sc} were confirmed in many systems of prion propagation, including cultured cells infected with prions (*17*−*20*).

Protease resistance and insolubility in detergents are now routinely used as surrogate markers to assign the isoform of a PrP species. To emphasize this dependence on biochemical criteria, some investigators denote the PrP isoforms as PrP-sen (protease-sensitive) and PrP-res (protease-resistant) (*21*). To separate between the PrP isoforms, two biochemical tests are usually performed, either alone or in concert: (i) High-speed centrifugation is used to pellet PrP^{Sc} (routinely used "standard conditions" are 100000*g* for 1 h at 4 °C). (ii) The sample is subjected to proteolysis to digest away PrP^{C}. For example, incubation with 10−40 μg/mL proteinase K at 37 °C for 1 h (the "standard proteolysis conditions") usually eliminates PrP^{C} completely while PrP^{Sc} is trimmed to form PrP27−30. Using these tests, an operational definition of bona fide PrP^{Sc} is achieved. Such tests are also at the basis of all current commercial kits for the detection of humans and animals infected with prions.

The question remains as to whether the operational classification of the PrP varieties based on proteolysis and sedimentation is accurate and complete. Several observations suggest that this may not be the case. For instance, inactivation of scrapie infectivity with ionizing radiation indicates a target size of about 55 kDa (*22*). This implies that the

† This work was supported by a generous grant from the Israel Ministry of Health.

* To whom correspondence should be addressed at the Department of Molecular Biology, The Hebrew University−Hadassah Medical School, P.O. Box 12272, Jerusalem 91120, Israel. Phone: +972-2-675-7105. Fax: +972-2-675-7086. Email: taraboul@cc.huji.ac.i.

‡ The Hebrew University−Hadassah Medical School.

§ Hadassah University Hospital.

[1] Abbreviations: GdnSCN, guanidine thiocyanate; NOG, *n*-octyl β-D-glucopyranoside; PrP^{C}, the normal isoform of the prion protein; PrP^{Sc}, the pathological isoform of the prion protein; TSE, transmissible spongiform encephalopathy.

10.1021/bi025958g CCC: $22.00
Published on Web 09/27/2002

minimal size of prions, or at least of their catalytically active propagation site, is about that of a PrP dimer. Such a small oligomer is not expected to sediment in the standard sedimentation conditions. In another study, Safar et al. (*23*) established a conformation-dependent immunoassay for PrP^{Sc} based on the enhanced immunoreactivity of this isoform after treatment with denaturing chaotropes (*24*). When homogenates of prion-infected brains were subjected to standard proteolysis conditions (proteinase K 20 μg/mL, 37 °C, 30 min) prior to the immunoassay, the denaturation-dependent signal was considerably weakened. This indicated that proteolysis eliminates a large amount of β-sheet-containing PrP^{Sc}, thus contradicting the standard operational definition of PrP^{Sc} as consisting exclusively of a protease-resistant isoform.

We now show that prion-infected brains and cells contain significant amounts of previously unrecognized protease-sensitive PrP^{Sc}. By gel filtration and sedimentation, these novel PrP^{Sc} species formed a continuum of aggregation sizes in both ionic and nonionic detergents. The protease-sensitive PrP^{Sc}-containing aggregates had a molecular mass as small as 600 kDa (i.e., less than 20 PrP molecules). While recognition of larger aggregates by PrP Abs depended on prior denaturation, the smallest PrP^{Sc} complexes were very immunoreactive in their native form (in contrast to "classical" protease-resistant PrP^{Sc}). Whether the smaller PrP^{Sc} aggregates are metabolic intermediates either in the synthesis or in the degradation of the classical PrP^{Sc} aggregates remains to be determined.

MATERIALS AND METHODS

Materials. Cell culture reagents were purchased from Biological Industries (Beit Haemek, Israel). Tissue culture plates were from Miniplast (Ein Shemer, Israel) or Nunc (Denmark). G418 (345810) and *n*-octyl β-D-glucopyranoside (NOG; 494459) were from Calbiochem (San Diego, CA). Secondary antibodies were from Jackson ImmunoResearch (PA). Other chemicals were from Sigma Chemical Co. (St. Louis, MO).

Cells and Tissues. N2a and ScN2a mouse neuroblastoma (*17*) and neurohypophyseal GT1-1 (*25*, *19*) cells have been described. N2a-C10 and ScN2a-C10 cells stably express the MHM2-PrP chimeric gene that carries the 3F4 epitope (*26*). Cells were maintained at 37 °C in DMEM16 supplemented with 10% fetal calf serum (FCS) (N2a) or 5% FCS and 5% horse serum (GT1).

Animals. Four-week-old outbred Syrian hamsters were inoculated intracerebrally with 50 μL of 10% brain homogenate (w/v) from a Syrian hamster terminally sick with Sc237 experimental scrapie (*27*). The animals were sacrificed at 80 days post-inoculation at a time when clinical signs of scrapie were evident. Brains were immediately homogenized in PBS (phosphate-buffered saline) to 10% w/v using a Ultra Turrax T8 IKA Labor Technik (Germany) homogenizer (settings: 10 000 rpm, 1 min, RT). The homogenates were then lysed (8 μL of homogenate was diluted to 200 μL with 2% NOG in HEPES buffer). Insoluble material was removed by a 30 s spin in an eppendorf centrifuge, and 200 μL supernatants were brought to 1% Sarkosyl (sodium sarcosinate) and incubated for 30 min on ice.

Antibodies. Rabbit antiserum R073 binds to both mouse PrP and MHM2-PrP. mAb 3F4 binds to residues Met_{108} and Met_{111} in the chimeric MHM2-mouse PrP but does not recognize the wild-type mouse PrP endogenous to N2a and ScN2a cells. Both antibodies were used at a dilution of 1:5000 (of the serum or the ascitic fluid).

PrP Isoforms and PrP Analysis. Characterization of the PrP isoforms by the standard criteria was carried out as described (*28*). Classical protease-resistant PrP^{Sc} was defined as the PrP fraction resistant to standard proteolysis catalyzed by proteinase K (20 μg/mL, 37 °C, 30 min for experiments with cultured cells, and 40 μg/mL, 37 °C, 1 h for experiments with brain samples). Proteolysis was terminated by the addition of phenylmethanesulfonyl fluoride (PMSF) to 2 mM. SDS−PAGE and western immunoblotting of the PrP isoforms were all carried out as described (*28*).

Velocity Sedimentation in Sucrose Gradients. The entire procedure was performed at 4 °C. Cells were scraped in ice-cold HEPES buffer (20 mM HEPES, pH 7.4, 150 mM NaCl, 0.1 mM $CaCl_2$, 1 mM $MgCl_2$), and then lysed for 30 min in HEPES buffer containing 2% NOG. Insoluble material was removed by a 30 s spin at 14 000 rpm in an eppendorf 5415C centrifuge, and 200 μL supernatants were brought to 1% Sarkosyl, incubated for 30 min on ice, and then loaded on top of 10−60% sucrose step gradients in TNS (10 mM Tris, pH 7.5, 150 mM NaCl, 1% Sarkosyl). Gradients were formed in a TLS-55 Beckman (Palo Alto, CA) Optima TL ultracentrifuge using Polyallomer (11 × 34 mm) tubes from 300 μL of each of the following sucrose concentrations: 10, 15, 20, 25, 30, and 60%. The gradients were spun for 1 h at 4 °C at 55 000 rpm ($g_{av} = 200000g$) in a TLS-55 rotor. Eleven fractions (180 μL each) were collected from the top of the tube.

Gel Filtration. Experiments were performed using either Sepharose CL-2B, Superdex 200 HR (Figure 3), or Sephacryl S-200 HR (results not shown) (Pharmacia, Uppsala, Sweden) beads in 1 × 30 cm columns. Chromatography was performed in an Äkta-FPLC apparatus from Pharmacia, at room temperature or at 6 °C (with similar results). Columns were loaded with 200 μL cell lysates (prepared as described above for the velocity sedimentation), and 1 mL fractions were collected. Dextran blue (molecular mass 2×10^6 Da), phenol red, thyroglobulin (molecular mass 6.69×10^5 Da), apoferittin (molecular mass 4.43×10^5 Da), and alcohol dehydrogenase (molecular mass 1.5×10^5 Da) served as molecular mass markers for the chromatography.

Denaturation-Dependent PrP Immunoreactivity. To measure the dependence of PrP immunoreactivity (in each gradient fraction) on protein denaturation, we used the dot-blot procedure described by Serban et al. (*24*) [see also (*23*)]. N2a and ScN2a as well as N2a-C10 and ScN2a-C10 cells were subjected to sucrose−Sarkosyl gradients as described above. From each fraction, *N*, of the gradients, 90 μL was loaded on prewetted nitrocellulose membranes (Schleicher & Schuell, Dassel, Germany). The membranes were rinsed briefly in TBST (150 mM NaCl, 10 mM Tris-HCl, pH 8, 0.3% Tween 20) and cut into strips. Strips were incubated for 5 min at RT with or without 3 M guanidine thiocyanate (GdnSCN) prepared in 50 mM Tris-HCl, pH 7.5. After extensive rinses in TBST, the strips were blocked with homogenized 1% fat milk and were then processed for immune detection using either the rabbit PrP antiserum R073 (N2a) or the mAb 3F4 (N2a-C10), followed by a secondary antibody conjugated to horseradish peroxidase. Blots were

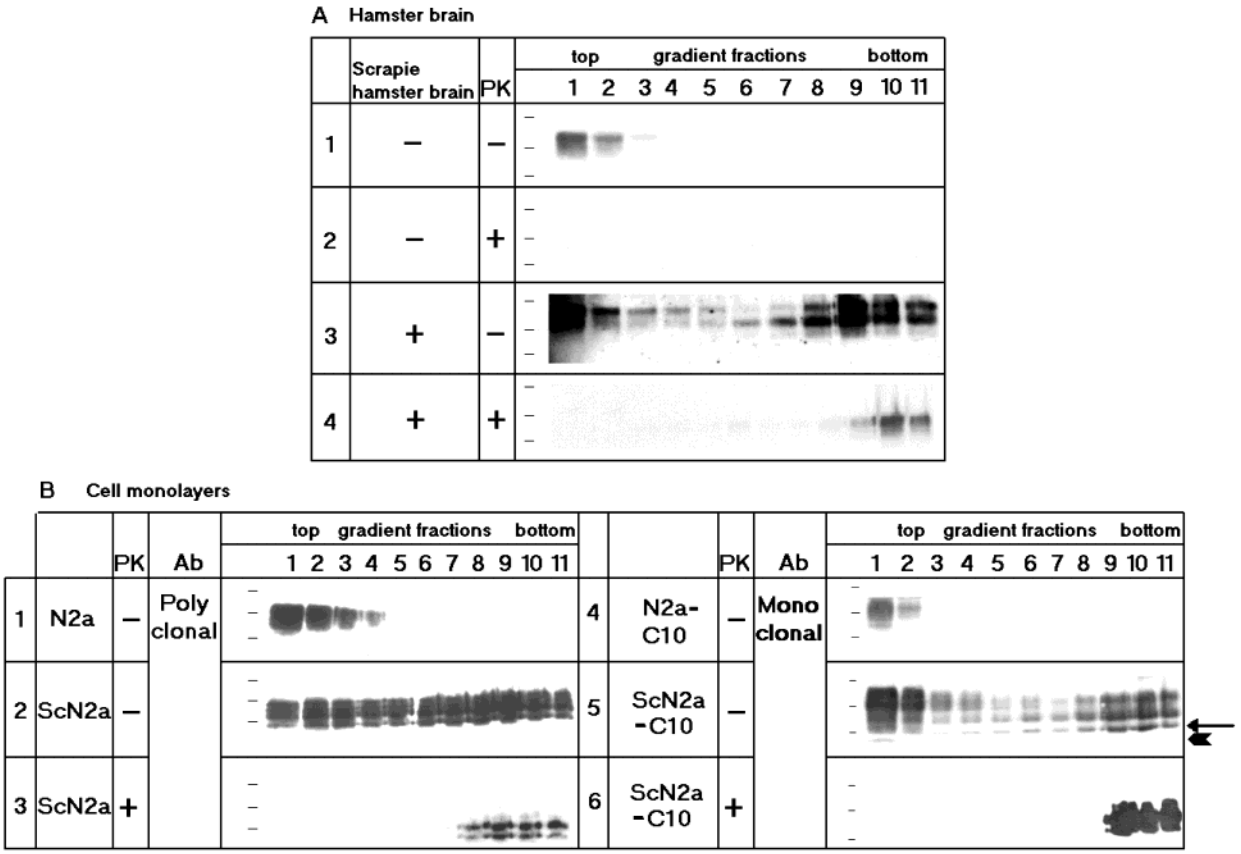

FIGURE 1: Small PrP^{Sc} aggregates in scrapie-infected cells and brains. Lysates of brains (panel A) and cells (panel B) were fractionated on 10−60% sucrose step gradients containing Sarkosyl, and the PrP content of the fractions was analyzed in Western immunoblots developed with either the rabbit PrP antiserum R073 (panel B, rows 1−3) or the mAb 3F4 (panel A and panel B, rows 4−6). Panel A: Ten percent (w/v) homogenates of brains uninfected (rows 1 and 2) and scrapie-infected hamster (80 d post-inoculation) were first lysed with 2% NOG and then brought to 1% Sarkosyl and incubated on ice for 30 min prior to analysis on sucrose gradients containing 1% Sarkosyl. In rows 2 and 4, the fractions were treated with proteinase K (40 μg/mL, 37 °C, 1 h) prior to immunoblotting. Panel B: Uninfected N2a (row 1) and N2a-C10 (row 4) and persistently infected ScN2a (rows 2 and 3) and ScN2a-C10 (rows 5 and 6) were lysed in 2% NOG. Postnuclear supernatants were made 1% with Sarkosyl, incubated for 30 min on ice, and analyzed in gradients containing 1% Sarkosyl. In rows 3 and 6, gradient fractions were digested with proteinase K (20 μg/mL, 37 °C, 30 min) prior to the electrophoresis. Of note, digesting PrP^{Sc} with proteinase K produced the PrP 27−30 glycoforms which have lost residues 24−90. The 17 kDa (arrowhead) and 19 kDa (arrow) bands, which are specific metabolites of PrP^{C} and PrP^{Sc}, respectively, are shown in row 5. The molecular markers indicated are 44, 28.8, and 18.5 kDa.

developed by chemiluminescence as described (*28*), and the immunoreactivity signals were quantitated by scanning densitometry using the TINA program from Raytest (Strauben, Hardt, Germany). Six independent experiments (three for each Ab) were used to generate the results shown in Figure 4.

The dependence of PrP immunoreactivity on GdnSCN-induced denaturation was calculated independently for each fraction, *N*, as follows: In the N2a cells, the dot-blot signal, $I^{N2a}{}_{N}$, somewhat decreases following incubation with GdnSCN. Since PrP^{C} immunoreactivity with R073 or 3F4 does not depend on denaturation (*23, 24*), this decrease was caused by a loss of PrP immunoreactive material from the membrane. The [GdnSCN] dependence of the PrP^{C} signal:

$$f(N) = I^{N2a}{}_{N,3M}/I^{N2a}{}_{N,0} \quad (1)$$

was then used to normalize the dot-blot intensities of fractions from ScN2a cells in the GdnSCN-treated blots. For each fraction, *N*, of ScN2a gradients, the dependence of PrP immunoreactivity on denaturation was thus

$$Y(N) = f(N)*I^{ScN2a}{}_{N,3M}/I^{ScN2a}{}_{N,0} \quad (2)$$

Thus, $Y = 1$ indicates PrP species that react equally well with Abs with or without denaturation. For ScN2a cells, *Y* strongly increased in faster sedimenting fractions (see Results, Figure 4).

RESULTS

Low Molecular Mass, Protease-Sensitive PrP Assemblies in Scrapie-Infected Cells and Brain. We asked whether PrP molecules might exist in prion-infected tissues that do not fall into either of the two 'canonical' PrP categories defined by the standard conditions of proteolysis and sedimentation (*14*). We first studied the aggregation pattern of the PrP isoforms in brains of scrapie-infected hamsters. Velocity sedimentation through sucrose gradients containing the ionic detergent Sarkosyl showed that PrP assemblies smaller than the "classical" protease-resistant PrP^{Sc} but larger than PrP^{C} exist in the scrapie-infected tissues but not in their uninfected counterparts (Figure 1A). Whereas PrP^{C} from normal brain (row 1) failed to sediment, PrP species from scrapie-infected brain spread throughout the gradients (row 3). Of the latter PrP species, only those that reached the bottom of the gradient (60% sucrose) partially resisted 'standard' proteoly-

sis (40 μg/mL, 37 °C, 1 h) (*14*) whereas species in fractions 1−9 were completely digested in these conditions.

We performed similar experiments with cultured cells infected with scrapie (Figure 1B). Mouse neuroblastoma N2a cells, their persistently infected subclone ScN2a (*17*), as well as variants of those cells that express the epitopically labeled MHM2-PrP which react with mAb 3F4 were analyzed on Sarkosyl−sucrose gradients. In all cases, PrP^{C} from uninfected cells failed to sediment (Figure 1B, rows 1 and 4). In contrast, infected cells yielded PrP bands throughout the gradient (Figure 1B, rows 2 and 5), but only the fast-sedimenting PrP aggregates resisted proteolysis (Figure 1B, rows 3 and 6). These results were obtained both with the PrP antiserum R073 (Figure 1B, rows 1−3) and with the mAb 3F4 (Figure 1B, rows 4−6).

Although the PrP species in fractions 3−9 (Figure 1A, row 3, Figure 1B, rows 2 and 5) were found exclusively in cells and tissues infected with prions, they differed from the standard PrP^{Sc} molecules in that (i) they did not resist 'standard' proteolysis, and (ii) they sedimented slower than protease-resistant PrP^{Sc} (but faster than PrP^{C}). Thus, these "nonstandard" PrP^{Sc} species were found in small assemblies and were protease-sensitive.

Because ScN2a is a clonal cell line (*17*) with overall properties largely different from uninfected N2a populations, we considered the possibility that a coincidental (non-prion-related) metabolic anomaly in these cells could lead to the aggregation of PrP^{C}. Aggregation of wt PrP can indeed be found in uninfected cells subjected to metabolic insults (*29*−*32*). To overcome this possible clonal problem, we turned to GT1-1 cells (*25*), which are very permissive to prion infection so that uncloned infected populations can be studied (*19*). We found that freshly infected ScGT1-1 cells (at the fourth passage after the infection) also contained small PrP^{Sc} aggregates in fractions 3−9 of sucrose gradients, in contrast to uninfected GT1-1 cells (Figure 2B). Finally, we noted that ScN2a-C10 cells that had spontaneously stopped producing PrP^{Sc} lost the slow-sedimenting PrP^{Sc} aggregates as well (not shown). Taken together, these results clearly show that the slow-sedimenting PrP^{Sc} species are induced specifically by prion infection. Similar species could also be demonstrated when Sarkosyl was replaced by less denaturing detergents such as NOG (Figure 2B) or Triton X-100−sodium deoxycholate (not shown) throughout the procedure. This shows that small PrP^{Sc} assemblies do not result from an artifactual denaturation of PrP by the anionic detergent Sarkosyl.

In cultured cells, PrP^{C} is degraded in two consecutive steps via a set of degradation intermediates (whose unglycosylated form has a molecular mass of 17 kDa) (*33*). In contrast, the N-terminal trimming of PrP^{Sc} by cellular acid hydrolases produces the protease-resistant PrP27−30 core, whose unglycosylated form has a molecular mass of 19 kDa. This 19 kDa protease-resistant core resists further degradation to the 17 kDa intermediates (*33*, *34*). The 17 and 19 kDa species are thus specific markers of PrP^{C} and PrP^{Sc} metabolism, respectively. In both infected and uninfected cells, the 17 kDa PrP bands were confined to the top two or three fractions of the gradients (arrowhead in Figure 1B, row 5, and Figure 2, rows 2), which thus contained primarily PrP^{C} and its metabolites. In contrast, fractions 3−11 comprise the 19 kDa band (arrow in row 8) and were thus in this sense comparable to PrP^{Sc}. Thus, the small PrP^{Sc} aggregates starting in fraction 3 possess a metabolically stable 19 kDa core, and are in this respect similar to PrP^{Sc}.

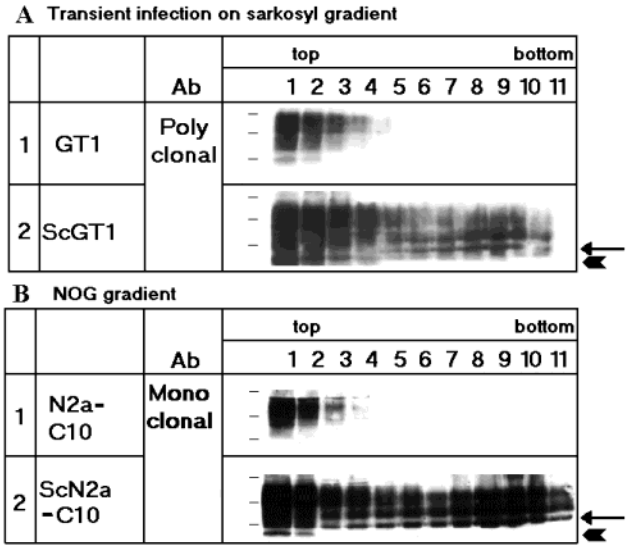

FIGURE 2: Small PrPSc aggregates are found within freshly infected cells as well as in *N*-octyl β-D-glucopyranoside containing gradients. Panel A: GT1-1 cells and freshly infected ScGT1-1 were lysed using 2% NOG, brought to 1% Sarkosyl, and incubated for 30 min on ice before analysis on a 10−60% sucrose step gradient containing 1% Sarkosyl. Panel B: N2a-C10 and ScN2a-C10 cells were lysed in 2% NOG and analyzed on a sucrose gradient containing 2% NOG (but no Sarkosyl). In both panels, arrows indicate the 19 kDa PrP27−30, and arrowheads indicate the 17 kDa intermediate. The molecular markers indicated are 44, 28.8, and 18.5 kDa.

The finding that slow sedimenting PrP aggregates exist in cell lysates reconciles the prion hypothesis with the previous finding of scrapie infectivity in similar fractions of sucrose gradients containing Sarkosyl (*35*).

Small Prion-Specific PrP-Containing Structures Confirmed by Gel Filtration. Because PrP species have a strong affinity for lipids, we had to ascertain that the slow sedimentation of the small PrP aggregates in sucrose gradients (Figure 1) indeed reflects their small size and not a possible buoyant density. The affinity of both PrP isoforms to cholesterol and glycolipid rafts is well established (*28*, *36*−*39*). Although both Sarkosyl and NOG solubilize rafts (*40*), PrP^{Sc} could be attached to abnormal membrane structures that behave differently than physiological membranes. Thus, prion rods purified from the brains of hamsters sick with experimental scrapie contain detectable amounts of sphingomyelin even after extensive extraction with detergents and chloroform−methanol (*41*). We therefore used gel filtration as an independent means to determine whether small PrP^{Sc} aggregates are found in scrapie-infected samples (Figure 3). Cells were lysed in 2% NOG, and postnuclear supernatants were brought to 1% Sarkosyl prior to chromatography, which was run at room temperature (6 °C runs or cell lysis in Triton-X-100−sodium deoxycholate instead of NOG gave similar results). We first used Sepharose CL 2B, with a cutoff molecular mass of ca. 4×10^7 Da, as a separation medium (Figure 3A). PrP^{C} from uninfected cells consistently emerged from Sepharose CL 2B columns in fractions 17−19 (row 1). In contrast, PrP from infected cells first exited the column with the excluded fraction (Figure 3A, fraction 6) and spread throughout the output of the column up to fraction 19 (Figure 3A, row 2). Dextran blue (molecular mass 2000 kDa) exited

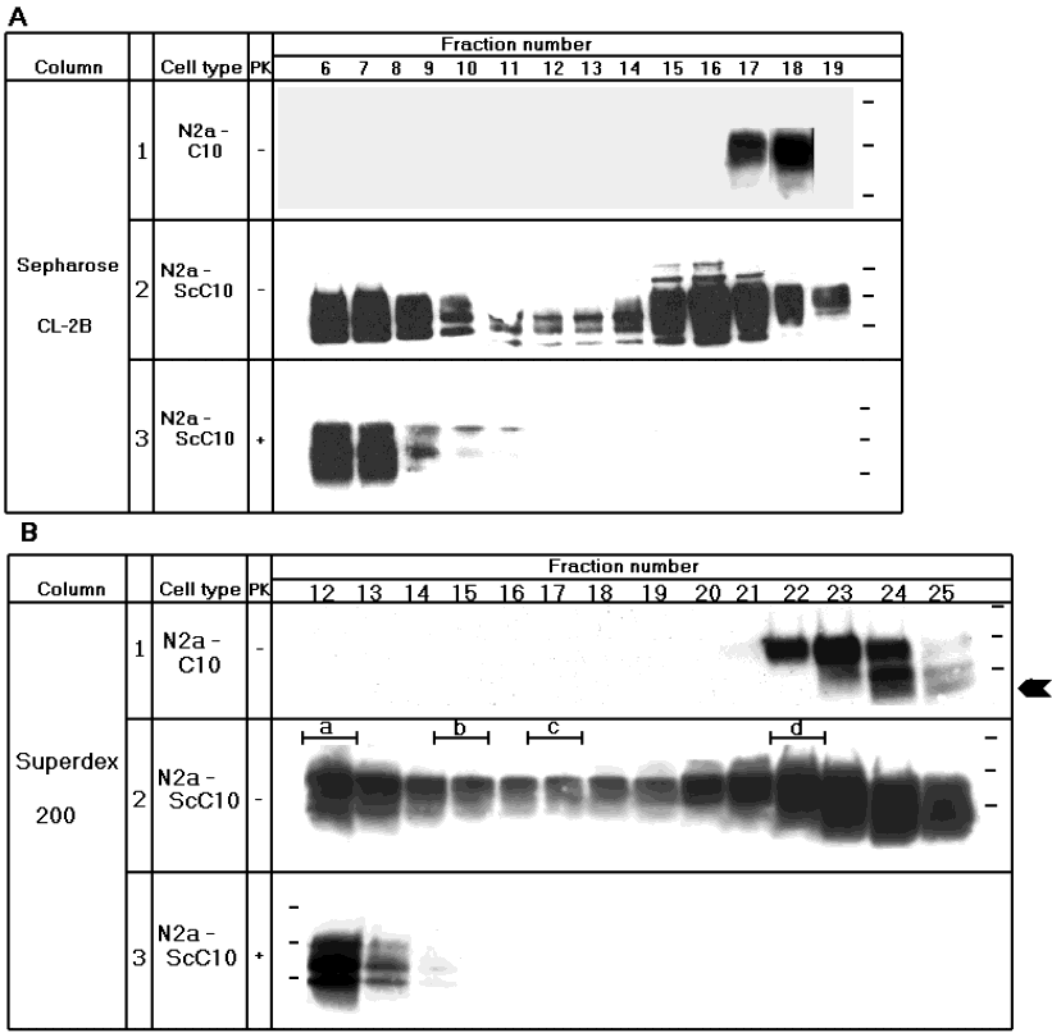

FIGURE 3: Small prion-specific, PrP-containing structures confirmed by gel filtration. N2a-C10 and ScN2a-C10 cells were lysed in 2% NOG. Postnuclear supernatants were made 1% with Sarkosyl and incubated on ice for 30 min, and then were fractionated on Sepharose CL-2B (panel A) or Superdex 200 HR 10/30 columns (panel B) which were run at RT in a buffer containing 1% Sarkosyl. The PrP content of the fractions was analyzed in western immunoblots developed with the mAb 3F4. In rows 3, the fractions were treated with proteinase K (20 μg/mL, 37 °C, 30 min) prior to immunoblotting. The arrowhead in Figure 2B, row 1, shows the 17 kDa intermediate. The elution peaks of molecular mass markers from the Superdex 200 HR 10/30 column are marked in panel B, row 2. The molecular mass markers used are: (a) dextran blue (ca. 2000 kDa), (b) thyroglobulin (669 kDa), (c) apoferritin (443 kDa), and (d) alcohol dehydrogenase (150 kDa). The SDS−PAGE molecular markers indicated are 44, 28.8, and 18.5 kDa.

the column in fractions 8 and 9 (not shown). PrP in fractions 6 and 7 partially resisted standard proteolysis and thus included standard protease-resistant PrP^{Sc} (Figure 3A, row 3), whereas the PrP species exiting later were sensitive to proteinase K. Thus, this matrix resolved intermediate-size PrP assemblies with a molecular mass between those of PrP^{C} and ca. 4×10^7 Da (the excluded volume). To achieve a more accurate size resolution of smaller PrP^{Sc}-containing assemblies, we used the smaller pore matrices Superdex 200-HR (dextran-based, cutoff molecular mass 600 kDa, Figure 3B) and Sephacryl S-200-HR (acrylamide-based, cutoff molecular mass 300 kDa) (results not shown). The columns were calibrated using the following molecular mass markers: dextran blue (2×10^6 Da), thyroglobulin (6.69×10^5 Da), apoferritin (4.43×10^5 Da), alcohol dehydrogenase (1.5×10^5 Da), and phenol red (3×10^2 Da) (Figure 3B, row 2). These columns resolved low molecular mass PrP^{Sc} aggregate species in structures as small as 600 kDa (Figure 3B, row 2), whereas both PrP^{C} and the 17 kDa (arrowhead) degradation intermediate were confined to the last three smallest fractions. As expected, monomers of the degradation intermediate, which is smaller than PrP^{C}, emerged last (fraction 25). Gel filtration data thus show that prion-specific PrP^{Sc} can exist in surprisingly small assemblies and not only as a part of large aggregates.

PrP Denaturation Profile. A hallmark of PrP^{Sc} is that its immunoreactivity is greatly augmented by denaturation (*20*, *24*), whereas PrP^{C} is unaltered in this respect [a possible exception is the mAb 15B3, which seems to interact well with native PrP^{Sc} (*42*)]. The reason for this denaturation-dependent immunoreactivity is unknown, but Ab recognition has been used to determine the denaturation profiles of PrP varieties in denaturing agents, as well as to estimate their β-sheets content (*23*, *43*).

To study the denaturation dependence of the immunoreactivity of PrP species separated by sucrose gradients, we used the dot-blot method of Serban et al. (*24*) (see Materials and Methods and Figure 4). Lysates from N2a and of ScN2a, as well as of N2a-C10 and ScN2a-C10 cells, were fractionated on sucrose−Sarkosyl gradients. Fractions were spotted on nitrocellulose strips that were then incubated either with or without 3 M GdnSCN prior to immunodetection with

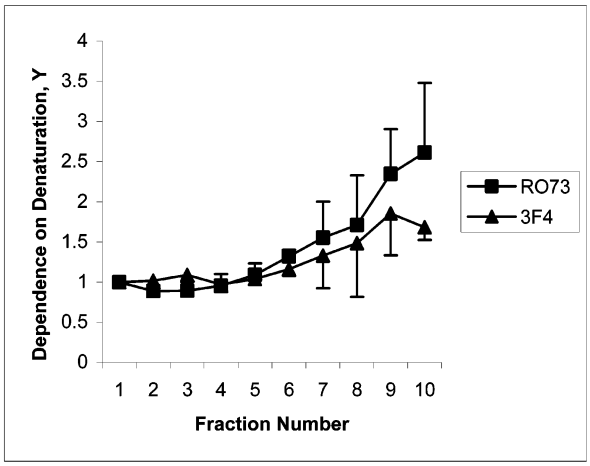

FIGURE 4: Prion characteristics of PrP^{Sc} in low molecular mass aggregates revealed by denaturation−immunoreactivity profile. Sucrose gradient fractions of N2a and ScN2a as well as N2a-C10 and ScN2a-C10 cells were dotted on nitrocellulose strips, which were then incubated with or without 3 M GdnSCN (5 min, RT) prior to immunodetection with R073 (N2a) or 3F4 (N2a-C10). Chemoluminescence intensities for the scrapie-infected cells were normalized using the PrP^{C} values of N2a and N2a-C10 cells, as explained in the text (see Materials and Methods). The dependence of immunoreactivity on denaturation (Y_N) was calculated independently for each fraction, *N*. The results are averaged from 6 independent experiments (3 experiments for each antibody).

R073 (ScN2a) or 3F4 (ScN2a-C10) (Figure 4). The signal intensity in each dot was measured by densitometry, and these values were used to determine the extent (Y_N) to which PrP in each fraction depends on GdnSCN denaturation for Ab recognition (see Materials and Methods). In this calculation, $Y = 1$ indicates PrP species that react equally well with Abs with or without denaturation, and increasing *Y* values indicate an increasing dependence on denaturation. *Y* increased sharply for heavier sucrose fractions (Figure 4). Thus, faster sedimenting fractions were increasingly dependent on denaturation. In this sense, PrP^{Sc} species in larger aggregates were increasingly similar to "classical" protease-resistant PrP^{Sc}. In contrast, PrP^{Sc} species in lighter fractions were immunoreactive without further denaturation, and thus were similar to PrP^{C}.

DISCUSSION

Using a variety of sizing techniques, we found that prion-specific PrP^{Sc} forms, in detergents, aggregates with sizes ranging from less than 600 kDa to a very large molecular mass. While small PrP^{Sc} aggregates were sensitive to proteolysis and were imunoreactive, as their size increased larger complexes progressively displayed the biochemical properties of "classical" protease-resistant PrP^{Sc}. That the low molecular mass aggregates contained PrP27−30 molecules suggests that their metabolism is similar to that of protease-resistant PrP^{Sc}. However, whether these low molecular mass PrP^{Sc} aggregates are metabolic intermediates in the formation or the degradation of the protease-resistant PrP^{Sc} species remains to be seen. Because the classical protease-resistant test fails to identify the novel PrP^{Sc} species, results from previous experiments that used this operational test will have to be reviewed. It will be interesting to see whether these protease-sensitive PrP^{Sc} species carry prion infectivity. We have inoculated protease-sensitive PrP^{Sc} fractions into animals. However, results are not expected before several months to more than a year. If these protease-sensitive PrP^{Sc} molecules are associated with prion infectivity, then these data should be incorporated in existing kits used for the veterinary detection of BSE, scrapie, and other prion diseases.

Two lines of evidence show that the small PrP aggregates are closely related to the classical PrP^{Sc} defined by resistance to proteolysis. First, they were found exclusively in prion-infected cells and brains. Second, PrP27−30 molecules (including the 19 kDa unglycosylated form), which are markers of the metabolism of PrP^{Sc} (*33*, *34*), cosedimented with these assemblies. In contrast, the 17 kDa band, which is an intermediate in the degradation of PrP^{C} but not of PrP^{Sc} (*33*), was found exclusively in fractions containing PrP^{C}. Taken together, these observations indicate that PrP^{Sc}, defined as the PrP molecules that appear exclusively during infection with prions, forms a continuum of aggregates of sizes ranging from less than 600 kDa (fractions 14−21 in Figure 3B) to that of rods [which can contain as many as 3×10^4 PrP molecules (*16*)]. These aggregates were observed in ionic (Sarkosyl), nonionic (NOG), and mixed (Triton X-100−sodium deochycholate) detergents.

We have not yet determined whether the smaller PrP^{Sc}-containing complexes are composed exclusively of PrP oligomers, or whether they also contain other chemical species with heterogeneous stoichiometry. Since PrP is a hydrophobic membrane molecule, detergent micelles are most probably attached to the PrP^{Sc} assemblies and are thus likely to contribute to the size measured by gel-filtration. Methods permitting better size resolution, such as nondenaturing gel electrophoresis, will have to be used to further characterize the small PrP^{Sc} assemblies. In a preliminary effort in that direction, we analyzed lysates from ScN2a-C10 and N2a-C10 cells by electrophoresis in Sarkosyl−polyacrylamide gradient gels (unpublished results). In the infected cells, but not in their uninfected counterparts, Western analysis of species separated on these gels detected a protease-sensitive immunoreactive smear presumably representing small PrP^{Sc} assemblies. However, we could detect no discrete PrP molecular mass ladder in these gels, suggesting either that PrP^{Sc} assemblies contain other molecules in varying stoichiometric ratios or that PrP^{Sc} possess heterogeneous electrophoretic properties, perhaps due to multiple conformations.

Our results are compatible with previous data suggesting that in some cases the infectious scrapie agent may assume small sizes and be sensitive to proteolysis. Measurement of the scrapie agent (performed before PrP was discovered) determined that scrapie infectivity might be found in fractions as small as 40 S, as determined in sucrose gradients (*35*). While the prion hypothesis dictates that these fractions should contain PrP^{Sc}, their size appears too small to accommodate the definition of PrP^{Sc} based on its pelleting properties at high speed. Similarly, agarose gel electrophoresis (also performed before the discovery of PrP, *44*) showed that some infectious prions migrated ahead of DNA fragments of ca. 10^6 Da in agarose gels in the presence of Sarkosyl. Small sizes of the scrapie agent were also hinted by the inactivation curves of scrapie infectivity by ionizing radiation, which indicated that the target size of the infectious site within the prion is as small as a PrP dimer (*22*).

A hallmark of PrP^{Sc} is that the immunoreactivity of this molecule depends vastly on prior denaturation (*24*). Safar et al. (*23*) have previously shown that this dependence correlates with the β-sheet content of PrP species. However, whether this conclusion holds for PrP^{Sc} species in the low molecular mass aggregates remains to be determined. If the correlation described by Safar et al. holds for these samples, then one would conclude that their β-sheet content is lower than that of "classical" protease-resistant PrP^{Sc}. Further work will be needed to establish the percentage of β-sheet in these samples using independent methods.

Several experiments with prions have been described where no PrP^{Sc} could be detected in infectious tissues (*45*, *46*). In all these cases, resistance to proteolysis was used to define PrP^{Sc}. Our findings raise the question of whether low molecular mass aggregates of protease-sensitive PrP^{Sc} may be involved in some of these cases. It will also be interesting to see if small aggregates are involved in prion models where PrP^{Sc} is very sensitive to proteolysis, such as in the *drowsy* strains of transmissible mink encephalopathy (*47*).

How are the small PrP^{Sc} assemblies metabolically related to the protease-resistant PrP^{Sc}? The data are consistent with at least three possibilities: First, the small PrP^{Sc} aggregates could be the metabolic precursor of classical protease-resistant PrP^{Sc}. Presumably, they are formed out of PrP^{C} molecules. Data collected from pulse−chase experiments in cultured cells indicate that protease-resistant PrP^{Sc} is formed very slowly ($t_{1/2}$ in ScN2a = 6 h) from a precursor that is 'indistinguishable' (using the standard criteria) from PrP^{C} (*48*). If the formation of protease-resistant PrP^{Sc} proceeds through small, protease-sensitive PrP^{Sc} assemblies, then this would indicate that prion-specific PrP is formed more rapidly than is currently assumed. Another possibility is that the small PrP^{Sc} assemblies are a degradation intermediate of protease-resistant PrP^{Sc}. That slow sedimenting fractions contain trimmed PrP27−30 variants of PrP (for instance, the 19 kDa band, Figure 1B) is compatible with this possibility. Finally, it is also possible that the low molecular mass PrP assemblies are 'off-pathway' species that, while specific to prion diseases, are not metabolically related to PrP^{Sc}, so that protease-sensitive and protease-resistant PrP^{Sc} varieties remain unmixed. Kinetic experiments will be needed to sort among these possibilities.

ACKNOWLEDGMENT

We thank Ehud Cohen and Esther Metzer for helpful discussions and Daphna Fuchs for technical help.

REFERENCES

1. Prusiner, S. B. (1982) *Science 216*, 136−144.
2. *Cold Spring Harbor Monograph Series* (1999) (Prusiner, S. B., Ed.) Vol. 38, Cold Spring Harbor Laboratory Press, Cold Spring Harbor, NY.
3. Prusiner, S. B., Scott, M. R., DeArmond, S. J., and Cohen, F. E. (1998) *Cell 93*, 337−348.
4. Weissmann, C. (1999) *J. Biol. Chem. 274* (1), 3−6.
5. Borchelt, D. R., Taraboulos, A., and Prusiner, S. B. (1992) *J. Biol. Chem. 267*, 16188−16199.
6. Kellings, K., Prusiner, S. B., and Riesner, D. (1994) *Philos. Trans. R. Soc. London B 343*, 425−430.
7. Stahl, N., Baldwin, M. A., Teplow, D. B., Hood, L., Gibson, B. W., Burlingame, A. L., and Prusiner, S. B. (1993) *Biochemistry 32* (8), 1991−2002.
8. Caughey, B. W., Dong, A., Bhat, K. S., Ernst, D., Hayes, S. F., and Caughey, W. S. (1991) *Biochemistry 30*, 7672−7680.
9. Pan, K. M., Baldwin, M., Nguyen, J., Gasset, M., Serban, A., Groth, D., Mehlhorn, I., Huang, Z., Fletterick, R. J., Cohen, F. E., and Prusiner, S. B. (1993) *Proc. Natl. Acad. Sci. U.S.A. 90* (23), 10962−10966.
10. Brown, D. R., Qin, K., Herms, J. W., Madlung, A., Manson, J., Strome, R., Fraser, P. E., Kruck, T., von Bohlen, A., Schulz-Schaeffer, W., Giese, A., Westaway, D., and Kretzschmar, H. (1997) *Nature 390* (6661), 684−687.
11. Stahl, N., Borchelt, D. R., Hsiao, K., and Prusiner, S. B. (1987) *Cell 51*, 229−240.
12. Bolton, D. C., McKinley, M. P., and Prusiner, S. B. (1982) *Science 218*, 1309−1311.
13. Bolton, D. C., McKinley, M. P., and Prusiner, S. B. (1984) *Biochemistry 23*, 5898−5906.
14. Meyer, R. K., McKinley, M. P., Bowman, K. A., Braunfeld, M. B., Barry, R. A., and Prusiner, S. B. (1986) *Proc. Natl. Acad. Sci. U.S.A. 83*, 2310−2314.
15. McKinley, M. P., Meyer, R., Kenaga, L., Rahbar, F., Cotter, R., Serban, A., and Prusiner, S. B. (1991) *J. Virol. 65*, 1440−1449.
16. Prusiner, S. B., McKinley, M. P., Bowman, K. A., Bolton, D. C., Bendheim, P. E., Groth, D. F., and Glenner, G. G. (1983) *Cell 35*, 349−358.
17. Butler, D. A., Scott, M. R. D., Bockman, J. M., Borchelt, D. R., Taraboulos, A., Hsiao, K. K., Kingsbury, D. T., and Prusiner, S. B. (1988) *J. Virol. 62*, 1558−1564.
18. Race, R. E., Fadness, L. H., and Chesebro, B. (1987) *J. Gen. Virol. 68*, 1391−1399.
19. Schätzl, H. M., Laszlo, L., Holtzman, D. M., Tatzelt, J., DeArmond, S. J., Weiner, R. I., Mobley, W. C., and Prusiner, S. B. (1997) *J. Virol. 71* (11), 8821−8831.
20. Taraboulos, A., Serban, D., and Prusiner, S. B. (1990) *J. Cell Biol. 110*, 2117−2132.
21. Caughey, B., Neary, K., Butler, R., Ernst, D., Perry, L., Chesebro, B., and Race, R. E. (1990) *J. Virol. 64*, 1093−1101.
22. Bellinger-Kawahara, C. G., Kempner, E., Groth, D. F., Gabizon, R., and Prusiner, S. B. (1988) *Virology 164*, 537−541.
23. Safar, J., Wille, H., Itri, V., Groth, D., Serban, H., Torchia, M., Cohen, F. E., and Prusiner, S. B. (1998) *Nat. Med. 4* (10), 1157−1165.
24. Serban, D., Taraboulos, A., DeArmond, S. J., and Prusiner, S. B. (1990) *Neurology 40*, 110−117.
25. Mellon, P. L., Windle, J. J., Goldsmith, P. C., Padula, C. A., Roberts, J. L., and Weiner, R. I. (1990) *Neuron 5*, 1−10.
26. Scott, M. R., Köhler, R., Foster, D., and Prusiner, S. B. (1992) *Protein Sci. 1*, 986−997.
27. Shaked, G., Taraboulos, A., and Gabizon, R. (1999) *J. Biol. Chem. 274* (25), 17981−17986.
28. Naslavsky, N., Stein, R., Yanai, A., Friedlander, G., and Taraboulos, A. (1997) *J. Biol. Chem. 272* (10), 6324−6331.
29. Yanai, A., Meiner, Z., Gahali, I., Gabizon, R., and Taraboulos, A. (1999) *FEBS Lett. 460* (1), 11−16.
30. Lehmann, S., and Harris, D. A. (1997) *J. Biol. Chem. 272* (34), 21479−21487.
31. Ma, J., and Lindquist, S. (1999) *Nat. Cell Biol. 1* (6), 358−361.
32. Yedidia, Y., Horonchik, L., Tzaban, S., Yanai, A., and Taraboulos, A. (2001) *EMBO J. 20* (19), 5383−5391.
33. Taraboulos, A., Raeber, A. J., Borchelt, D. R., Serban, D., and Prusiner, S. B. (1992) *Mol. Biol. Cell 3*, 851−863.
34. Caughey, B., Raymond, G. J., Ernst, D., and Race, R. E. (1991) *J. Virol. 65*, 6597−6603.
35. Prusiner, S. B., Garfin, D. E., Cochran, S. P., McKinley, M. P., and Groth, D. F. (1980) *J. Neurochem. 35*, 574−582.
36. Gorodinsky, A., and Harris, D. A. (1995) *J. Cell Biol. 129* (3), 619−627.
37. Harmey, J. H., Doyle, D., Brown, V., and Rogers, M. S. (1995) *Biochem. Biophys. Res. Commun. 210* (3), 753−759.
38. Taraboulos, A., Scott, M., Semenov, A., Avrahami, D., Laszlo, L., Prusiner, S. B., and Avraham, D. (1995) *J. Cell Biol. 129* (1), 121−132.
39. Vey, M., Pilkuhn, S., Wille, H., Nixon, R., DeArmond, S. J., Smart, E. J., Anderson, R. G. W., Taraboulos, A., and Prusiner, S. B. (1996) *Proc. Natl. Acad. Sci. U.S.A. 93*, 14945−14949.

40. Brown, D. A., and Rose, J. K. (1992) *Cell 68*, 533−544.
41. Klein, T. R., Kirsch, D., Kaufmann, R., and Riesner, D. (1998) *Biol. Chem. Hoppe-Seyler 379* (6), 655−666.
42. Korth, C., Stierli, B., Streit, P., Moser, M., Schaller, O., Fischer, R., Schulz-Schaeffer, W., Kretzschmar, H., Raeber, A., Braun, U., Ehrensperger, F., Hornemann, S., Glockshuber, R., Riek, R., Billeter, M., Wuthrich, K., and Oesch, B. (1997) *Nature 390* (6655), 74−77.
43. Peretz, D., Williamson, R. A., Kaneko, K., Vergara, J., Leclerc, E., Schmitt-Ulms, G., Mehlhorn, I. R., Legname, G., Wormald, M. R., Rudd, P. M., Dwek, R. A., Burton, D. R., and Prusiner, S. B. (2001) *Nature 412* (6848), 739−743.
44. Prusiner, S. B., Groth, D. F., Bildstein, C., Masiarz, F. R., McKinley, M. P., and Cochran, S. P. (1980) *Proc. Natl. Acad. Sci. U.S.A. 77*, 2984−2988.
45. Hsiao, K. K. (1994) *Ann. N.Y. Acad. Sci. 724*, 241−245.
46. Lasmezas, C. I., Deslys, J. P., Robain, O., Jaegly, A., Beringue, V., Peyrin, J. M., Fournier, J. G., Hauw, J. J., Rossier, J., and Dormont, D. (1997) *Science 275* (5298), 402−405.
47. Bessen, R. A., and Marsh, R. F. (1992) *J. Virol. 66*, 2096−2101.
48. Borchelt, D. R., Scott, M., Taraboulos, A., Stahl, N., and Prusiner, S. B. (1990) *J. Cell Biol. 110*, 743−752.

BI025958G